ELSEVIER

Journal of Nuclear Materials 318 (2003) 151–156

journal of nuclear materials

www.elsevier.com/locate/jnucmat

The effect of mean stress on the fatigue behavior of 316 LN stainless steel in air and mercury

J.P. Strizak *, L.K. Mansur

Oak Ridge National Laboratory, Technology Group, Carbon and Insulation Materials, Bethel Valley Road, P.O. Box 2008, Oak Ridge, TN 37831-6088, USA

Abstract

Design of the mercury target system components for the spallation neutron source (SNS) requires data on high- and low-cycle fatigue behavior. The research and development program in progress includes determining the effects of mercury on the fatigue behavior of type 316 LN stainless steel, the primary material of choice for the target vessel. Uniaxial, load-controlled, fully reversed tension–compression $R = -1$ (minimum stress/maximum stress) fatigue tests have been conducted in air and mercury at room temperature employing constant amplitude sinusoidal loading at frequencies from 0.2 to 10 Hz. Stress amplitude versus fatigue life data (S–N curves) for both air and mercury show a sharp knee at approximately 1 million cycles indicating a fatigue endurance limit in either air or mercury around 240 MPa. Tensile mean stress ($R = 0.1$) lowers the endurance limit to 160 MPa. Lower frequency and mercury environment had some impact (degradation) on fatigue life of type 316 LN stainless steel at high stress levels (i.e., stresses considerably above the apparent fatigue limit). Test results for high mean stress conditions ($R = 0.3$, 0.5, and 0.75) at a cyclic frequency of 10 Hz exhibited further reductions in the endurance limit.

1. Introduction

The target material for the spallation neutron source (SNS) that is under construction at the Oak Ridge National Laboratory in the United States will be liquid mercury that is contained within a type 316 LN SS vessel. The mercury target container will be subjected to a variety of loading conditions in this application and structural design criteria for the target system have been developed which require a consideration of cyclic stresses during service [1]. In support of the data needs, an experimental program is underway to determine the fatigue properties of type 316 LN SS in both air and mercury and for both high- and low-cycle regimes. Previously [2], screening tests (fully reversed, load control fatigue) conducted in air and mercury at room temperature using a sinusoidal waveform indicated a reduction (2–3 times) in fatigue life in mercury at high-stress amplitudes, but showed no significant effect on high-cycle fatigue strength at low-stress levels. Furthermore, examination of the fractures for the higher stress levels in mercury revealed secondary cracking and little evidence of ductility. If mercury wets the freshly cracked surfaces during fatigue testing and crack growth rate is accelerated (a form of liquid metal embrittlement), such effects could be exacerbated in some ranges of the experimental parameters.

Generally, when investigating environmental effects, stress amplitude is not the only factor affecting material/environment interaction. Time-dependent environmental effects can also be of importance. When failure occurs by environmental fatigue, stress-cycle frequency, stress-waveshape, and mean stress can synergistically affect the cracking process. The frequency dependence of environmental fatigue is generally thought to result from the fact that interaction of a material and its environment is essentially a rate-controlled process. Low

* Corresponding author. Tel.: +1-865 574 5117; fax: +1-865 576 8424.

E-mail address: strizakjp@ornl.gov (J.P. Strizak).

0022-3115/03/$ - see front matter © 2003 Elsevier Science B.V. All rights reserved.
doi:10.1016/S0022-3115(03)00121-1

frequencies, when there is substantial elapsed time between changes in stress levels, allow time for interaction between material and environment; high frequencies do not. At very high frequencies, or under loading conditions resulting in high plastic strains, self-heating can occur that may affect fatigue behavior. Self-heating is normally not considered to an environmental fatigue phenomenon, and experimental design can reduce the temperature in order to isolate true environmental effects. Self-heating was not encountered in the specific results presented herein. When environments have a deleterious affect on fatigue behavior, a critical range of frequencies of loading may exist in which mechanical/environmental interaction is significant. Above this range the effect may disappear.

Initial observations on the impact of these various factors on the fatigue behavior of type 316 LN stainless steel appear elsewhere [3] and in the proceedings of the 4th International Workshop on Spallation Materials Technology (IWSMT-4) [4]. Recent data on the effects of high-frequency (up to 700 Hz) on the environmental fatigue behavior of the 316 LN material can be found elsewhere in the proceedings of this 5th International Workshop on Spallation Materials Technology (IWSMT-5) [5]. The effects of high mean stress loading conditions are presented herein.

2. Experimental

2.1. Material, specimens, and testing equipment

A single heat of as-received solution annealed annealed type 316 LN stainless steel was used for the fatigue tests. The 25 mm thick plate from which the specimens were machined met the American Society for Testing and Materials (ASTM) specification A240-88C, and the composition and relevant physical and tensile properties of this low-carbon, nitrogen-containing material are shown in Table 1. Additional information regarding the general microstructure, tensile properties, and strain-controlled low-cycle fatigue properties is recorded elsewhere [6].

Fatigue test specimens with a uniform-gage test section were machined parallel to the primary rolling direction of the 25 mm plate. Since specimen preparation can strongly influence resultant fatigue data, particular attention was given to surface preparation in the gage section of the specimens. Low stress grinding was employed to minimize residual stresses on the surface, and longitudinal polishing to remove radial machining marks resulted in a maximum surface roughness of 0.2 μm. The test specimen geometry used for low-frequency tests ($\leqslant 10$ Hz) described in this paper is shown in Fig. 1. To hold mercury around the test section of the specimen, a vial machined from commercially pure nickel was press-fit to the lower end of the specimen. The other end of the specimen was fitted with a bushing having the same outside diameter as the vial to facilitate gripping in the Instron 8500 fatigue machine. The assembly (see Fig. 2) was then ultrasonically cleaned and then filled with mercury prior to being loaded in the hydraulically-actuated collet type grips of the fatigue machine.

Table 1
Composition and relevant physical and tensile properties for type 316 LN stainless steel

Element	Wt%
C	0.009
Mn	1.75
P	0.029
S	0.002
Si	0.39
Ni	10.2
Cr	16.31
Mo	2.07
Co	0.16
Cu	0.23
N	0.11
Fe	Balance
Room temperature tensile properties:	
Strain rate	8×10^{-5}/s
0.2% offset yield strength	259.1 MPa
Ultimate tensile strength	587.5 MPa
Elongation	86.2%
Reduction in area	88.1%
Grain size	ASTM 3.7

2.2. Testing procedures

Constant amplitude, uniaxial load-controlled fatigue tests were conducted under several loading conditions defined by R ratio where $R = S_{\min}/S_{\max}$, the ratio of the applied minimum and maximum stresses (Fig. 3). Fully reversed tension–compression ($R = -1$) and tensile mean stress ($R = 0.1$, 0.3, 0.5, and 0.75) tests were con-

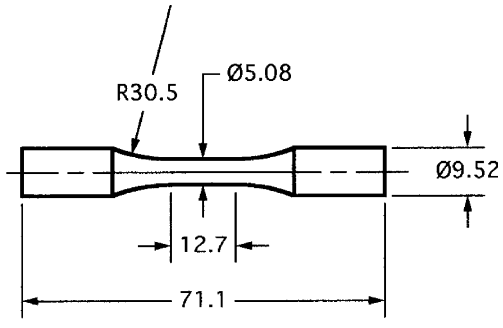

Fig. 1. Uniform-gage fatigue specimen.

Fig. 2. Fatigue specimen with bushing and vial for containment of mercury.

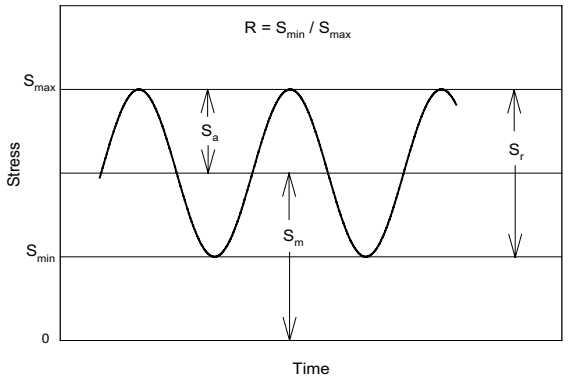

Fig. 3. Nomenclature for cyclic-stress testing.

ducted at room temperature, in air and mercury environments, generally employing a sinusoidal waveform over the frequency range 0.1–10 Hz.

Procedures for performing the load-controlled fatigue tests generally followed American Society for Testing and Materials (ASTM) guidance found in ASTM Standard E466, 'Standard Practice for Conducting Constant Amplitude Axial Fatigue Tests of Metallic Materials' [7].

3. Data interpretation and evaluation

Generally, load-control fatigue test results are plotted in terms of alternating stress, S_a, versus cycles to failure (N_f), the familiar S–N curve. In Fig. 3, $S_a = (S_{max} - S_{min})/2$. The number of cycles of stress that a metal can endure before failure occurs increases with decreasing stress. For some engineering materials, such as low-strength steel and titanium, the S–N curve becomes horizontal at low stresses. Below this limiting stress, known as the fatigue limit or endurance limit, the material is generally not observed to fail.

Other materials, including 316 stainless steel [8], do not exhibit a single-valued fatigue limit. Rather, the S–N curve continues to drop asymptotically, and for such behavior, a fatigue strength for a specific number of cycles is reported, i.e., the fatigue endurance limit depends upon the required cycles.

For design purposes it is useful to know how mean stress, S_m, affects the allowable alternating stress amplitude for a given life requirement. In Fig. 3, $S_m = (S_{max} + S_{min})/2$. At zero mean stress, the allowable stress amplitude is the effective fatigue limit for a specified fatigue life. As the mean stress increases, the permissible amplitude decreases. And, at a mean stress equal to the ultimate tensile strength of the material, the allowable cyclic amplitude is zero.

Two of the most widely used empirical relationships for describing the effect of mean stress on fatigue strength are shown in Fig. 4. The straight line joining the alternating fatigue strength at $R = -1$, S, for a given life to the ultimate tensile strength, S_u of the material is the Goodman law which is, as a rule-of-thumb, applicable to brittle materials but conservative for ductile materials. Gerber's law provides a parabolic relationship between S and S_u which is generally applicable to ductile materials. Many common materials exhibit mean stress effects that lie between the two empirical relationships.

In general, fatigue strength is dependent on a number of parameters including stress-cycle frequency, stress-waveshape, temperature, and mean stress (R-ratio). If environment is deleterious to fatigue behavior, there is generally a synergistic relationship between the environment and these parameters [9]. Degradation of the fatigue strength of a metal results from the enhanced initiation and propagation of cracks under the combined action of cyclic loading and environment.

4. Results and discussion

Plots of stress amplitude versus fatigue life (S–N plots), Figs. 5 and 6, show results in both air and mercury for fully-reversed tension–compression cyclic loading ($R = -1$), and a tensile mean loading condition

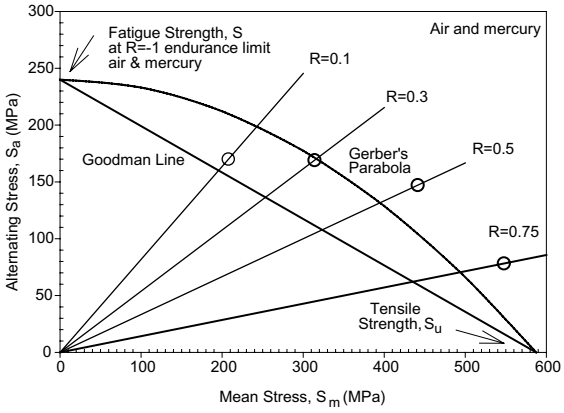

Fig. 4. Constant life diagram for type 316 LN stainless steel at 10 Hz in air and mercury for cyclic lives $>10^6$ (endurance limit).

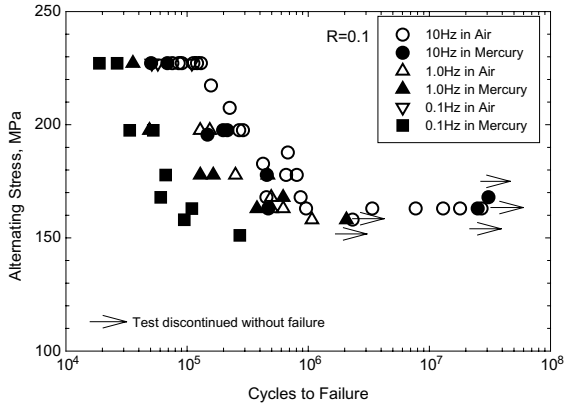

Fig. 6. Fatigue data for type 316 LN stainless steel in air and mercury for $R = 0.1$.

described by $R = 0.1$, respectively. A sharp knee in the data for $R = 0.1$ (Fig. 6) is observed at approximately 1 million cycles. Based on the available data out to 30 million cycles, the S–N data level off indicating a specific fatigue endurance limit for each R-ratio. Mercury reduced fatigue life, particularly at high stress amplitudes and at low frequencies. However, fatigue life near the endurance limit appears to be converging for the different frequencies. Limited data in Fig. 5 suggest that an endurance limit exists for fully reversed loading with $R = -1$.

At relatively low frequencies, both the loading frequency and the environment (mercury) had some impact on fatigue life of type 316 LN stainless steel at high-stress levels (i.e., stresses considerably above the apparent fatigue limit). For $R = 0.1$, those data in air and mercury are plotted separately in Figs. 7 and 8, respectively, to better differentiate the effect of frequency. At 10 Hz, fatigue lifetimes in mercury were less than those measured in air by approximately a factor of 2 at stress levels higher than the apparent fatigue limit. Furthermore, when the test frequency was lowered to 0.1 Hz, the resultant reduction in fatigue life in mercury was significantly greater than was observed in air. Fatigue lifetimes in mercury at 0.1 Hz were found to be approximately 70% lower than those at 10 Hz in mercury and nearly an order of magnitude lower than the results in air at 10 Hz.

This comparison (Figs. 7 and 8) reveals a synergistic relationship between decreasing cyclic loading frequency and mercury contributing to the degradation in fatigue life. The data also suggest that at the lowest frequency of 0.1 Hz mercury may even reduce the fatigue limit. Further tests at low stress amplitudes at such a low frequency would be very time consuming and, therefore, are not currently planned.

The process of fatigue consists of crack initiation at the surface of the test specimen, followed by progressive

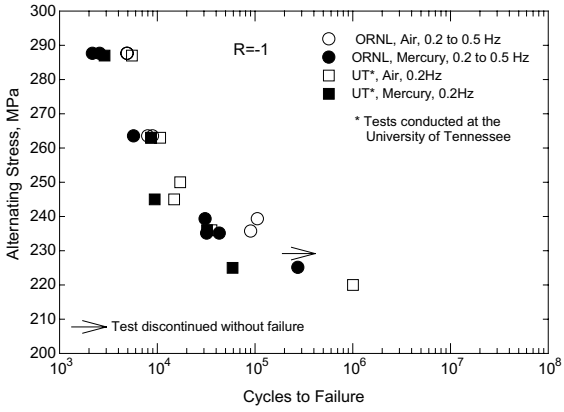

Fig. 5. Fatigue data for type 316 LN stainless steel in air and mercury for $R = -1$.

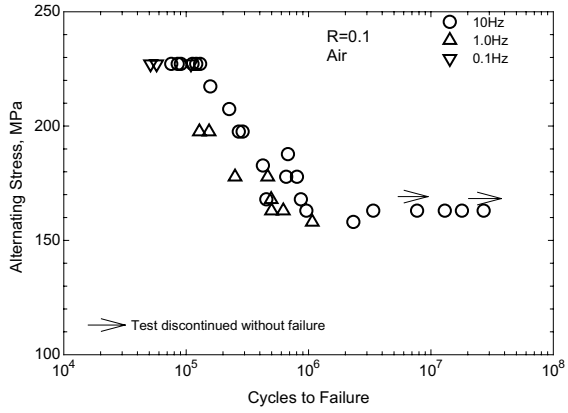

Fig. 7. Effect of frequency on fatigue life of type 316 LN stainless steel in air for $R = 0.1$.

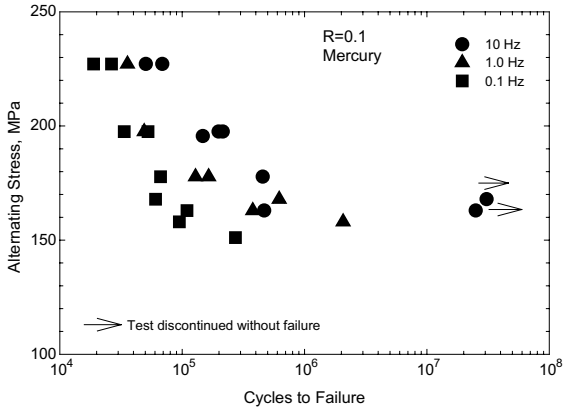

Fig. 8. Effect of frequency on fatigue life of type 316 LN stainless steel in mercury for $R = 0.1$.

cyclic growth of a crack until the remaining uncracked cross-section becomes too weak to sustain the loads imposed and abrupt fracture occurs. Fracture surfaces of specimens exposed to mercury [2] were completely wetted by the mercury while the remaining surface along the specimen gage area was not wetted. Since wetting is essential to liquid metal embrittlement, this suggests that there is likely no effect of mercury on crack initiation, but mercury apparently enhances crack propagation rates, and consequently lowers fatigue life.

A few fracture surfaces were examined previously [2] in a scanning electron microscope. For a high-stress amplitude, the specimen tested in mercury appeared to be much more brittle with widespread intergranular cracking, suggesting that liquid metal embrittlement occurred in mercury. At a low-stress amplitude near the fatigue endurance limit, fracture surfaces in mercury and air were more similar.

The frequency effect on fatigue life over the range 0.1–10 Hz is more pronounced in mercury (Fig. 8) than in air (Fig. 7). Since wetting by mercury is likely to be enhanced in a freshly formed crack, it might be expected that liquid metal embrittlement effects would result in a more significant (synergistic) frequency effect in mercury compared with air. However, the effect has been observed [4] to nearly disappear between 10 and 700 Hz when stress dependent test temperature (self-heating) encountered during high frequency load cycling was controlled.

For fully-reversed, zero mean stress, $R = -1$ cyclic loading, the S–N data in Fig. 5 level off indicating a fatigue endurance limit in either air or mercury around 240 MPa, the alternating stress amplitude below which fatigue failure will not occur. This value along with the reported tensile strength of the type 316 LN stainless steel was used to construct the constant-life diagram given in Fig. 4, used here to show the effect of mean stress on the endurance limit for the 316 LN material. In general, mean stress is detrimental to fatigue life. Fig. 9 shows that the allowable stress amplitude to achieve the given fatigue life is expected to decrease as mean stress increases.

When the loading cycle incorporates a tensile mean stress described by $R = 0.1$, the observed endurance limit (See Fig. 6) is reduced to 170 MPa. The experimental observation lies near the Goodman prediction shown in Fig. 4. Continuing, S–N data for $R = 0.3$ is given in Fig. 9. Though the mean stress is higher, the alternating stress (Fig. 4) is nearly the same as for the $R = 0.1$ condition. The experimental observation is higher than predicted by the Goodman Line, but lies near the Gerber Parabola.

S–N data for still higher mean stress conditions with $R = 0.5$ and 0.75 are shown in Figs. 10 and 11, respectively. The endurance limits decreased with increasing

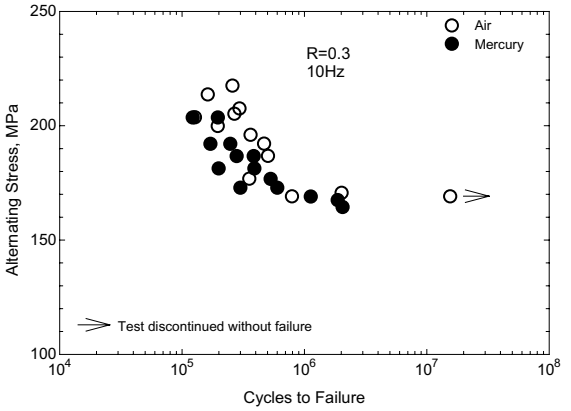

Fig. 9. Fatigue data for type 316 LN stainless steel for $R = 0.3$.

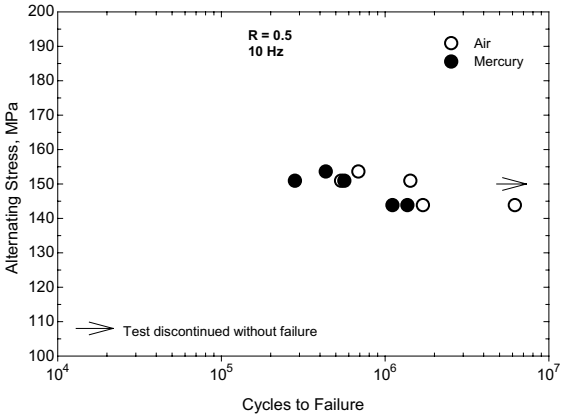

Fig. 10. Fatigue data for type 316 LN stainless steel for $R = 0.5$.

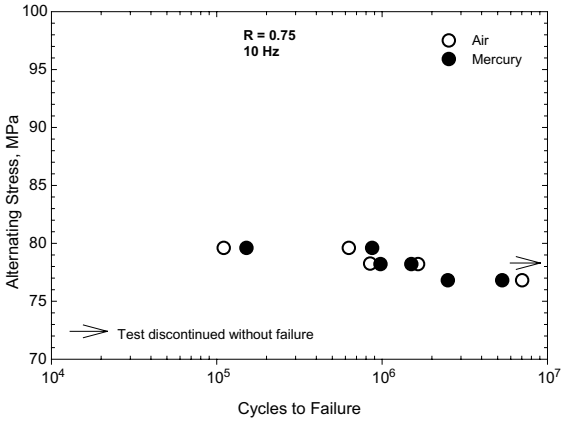

Fig. 11. Fatigue data for type 316 LN stainless steel for $R = 0.75$.

mean stress as expected, but, in both cases, the experimentally determined alternating stress was higher than predicted by either of the commonly used empirical relationships (Fig. 4). Normally, $R = 0.5$ and especially $R = 0.75$ are not applicable to design because the alternating stresses (Fig. 4) exceed the yield strength of the material. But the data could be useful in analyzing off-normal conditions.

5. Summary

S–N fatigue data have been obtained for type 316 LN stainless steel at room temperature for fully reversed, zero mean stress ($R = -1$) cyclic loading and for various tensile mean stress conditions with $R = 0.1$ to as high as $R = 0.75$. For load cycle frequencies over the range 0.1–10 Hz, mercury was deleterious to fatigue life. Generally, as frequency decreased, fatigue life decreased in the low-cycle region. However, fatigue life near the endurance limit in the high cycle region ($>10^6$ cycles) appears to converge for the different frequencies and for air and mercury environments. As expected, tensile mean stress reduces the endurance limit. The alternating stress required to achieve $>10^6$ cycles generally decreased with increasing R-ratio. For mean stress conditions defined by $R = 0.1$ and 0.3, the experimentally determined alternating stress at the endurance limit lie within the range predicted by commonly used empirical relationships, namely, the Goodman Line and the Gerber Parabola. At higher mean stress conditions defined by R-ratios of 0.5 and 0.75, both empirical relationships, particularly the Goodman Line underestimated the experimentally determined endurance limits. These key results for 10 Hz in air and mercury are shown in Fig. 4.

Acknowledgements

Research was sponsored by the Office of Science, US Department of Energy, under contract no. DE-AC05-00OR22725 with UT-Battelle, LLC.

References

[1] G.T. Yahr, C.R. Luttrell, SNS/TSR-181, UT-Battelle, LLC, Oak Ridge National Laboratory, 5 April 2000.
[2] S.J. Pawel, J.R. DiStefano, J.P. Strizak, C.O. Stevens, E.T. Manneschmidt, ORNL/TM-13759, SNS/TSR-0097, Lockheed Martin Energy Research Corporation, Oak Ridge National Laboratory, March 1999.
[3] J.P. Strizak, J.R. DiStefano, ORNL/TM-2000/270, UT-Battelle, LLC, Oak Ridge National Laboratory, October 2000.
[4] J.P. Strizak, J.R. DiStefano, P.K. Liaw, H. Tian, J. Nucl. Mater. 296 (2001) 225.
[5] H. Tian, P.F. Liaw, J.P. Strizak, L.K. Mansur, J. Nucl. Mater., these Proceedings. doi:10.1016/S0022-3115(03)00116-8.
[6] R.W. Swindeman, ORNL/NPR-92/94, Martin Marietta Energy Systems, Incorporated, Oak Ridge National Laboratory, June 1993.
[7] ASTM Standard E466, Annual Book of ASTM Standards, vol. 03.01, American Society for Testing and Materials, Metals Park, OH.
[8] ASME Boiler and Pressure Vessel Code, Section III, Division I, American Society of Mechanical Engineers, New York, 1995.
[9] ASM Handbook, vol. 19, Fatigue and Fracture, ASM International, Metals Park, OH, 1996.